Synergistic surface treatments for sustainable recycled aggregate concrete: experimental performance and machine learning prediction of compressive strength with an interactive online interface

sustainability

MDPI

Article

Synergistic Surface Treatments for Sustainable Recycled Aggregate Concrete: Experimental Performance and Machine Learning Prediction of Compressive Strength with an Interactive Online Interface

Marwah Al tekreeti * and Ali Bahadori-Jahromi

Department of Civil Engineering and Built Environment, School of Computing and Engineering, University of West London, London W5 5RF, UK; ali.bahadori-jahromi@uwl.ac.uk

* Correspondence: marwah.altekreeti@uwl.ac.uk

Abstract

Recycled concrete aggregate (RC A) is considered a sustainable material; however, its porosity and interfacial properties are poor due to adhering mortar. This study investigates the influence of synergistic surface treatments in terms of improving RCA quality and the resulting compressive strength of recycled aggregate concrete (RAC). A machine learning (ML) model was also developed to predict the compressive strength of recycled aggregate concrete (RAC) with different surface treatments, not just untreated RCA. In this study, three different RCA surface treatments were investigated. In this regard, acetic acid, silica fume, and sodium silicate treatments were combined. The properties of concrete and fresh concrete were investigated using slump and compressive tests at 28 and 90 days. The performance of various ML models, incorporating Gradient Boosting, Random Forest, XGBoost, and Extra Trees, was investigated. The performance of different models was also evaluated using R^2, MAE, and RMSE. SHAP analysis was used to evaluate the performance of different models. It has been observed that the use of surface treatment leads to lower water absorption values and higher interfacial bonding, as well as substantial improvements in compressive strength. Specifically, the use of acetic acid and silica fume for treating RCA produced compressive strengths similar to those achieved from natural aggregates at lower costs. XGBoost has the highest accuracy among all models. The R^2 value of XGBoost was 0.909. The SHAP analysis indicates that cement and curing age are the main features. RCA treatment parameters are considered modifiers. A user-friendly online tool was created to estimate compressive strength using different types of RCA treatment. The RCA treatment with sodium silicate and silica fume performed best in terms of embodied carbon among the treated mixes; it was deemed the best alternative from an environmental standpoint.

Keywords: recycled aggregate concrete; treatment; machine learning; spraying treatment; hybrid treatment; life cycle assessment

Academic Editor: José Ignacio Alvarez

Received: 26 February 2026

Revised: 31 March 2026

Accepted: 1 April 2026

Published: 3 April 2026

1. Introduction

The construction industry has been primarily responsible for consuming the largest quantities of natural resources, driven by rapid urban growth. Concrete is the most widely used construction material, followed by water. The quantity of concrete produced is 14 billion tons annually [1]. The high quantity of concrete produced has a direct correlation with environmental impacts such as the emission of CO_2, the consumption of non-renewable resources, the destruction of habitats, and the generation of waste. The quantity of construction and demolition waste produced in the United Kingdom in 2022 was 59.4 million tons [2]. This indicates that a considerable portion of construction waste generated within the UK is landfilled, and the global problem of excessive C&D waste being landfilled is especially problematic in major urban centers. As such, the use of RCA provides an additional material choice to help minimize the quantity of construction waste generated and improve the sustainability of natural resources used in construction; however, the quality issues associated with RCA (containing residual mortar, increased porosity, and micro-cracks) (Figure 1) limit its mechanical performance relative to that of natural aggregate [3–5].

Figure 1. Raw RCA.

Many different methods have been tested for pretreating RCA, including removal, [6], the enhancement of adhered mortar (AM) [7–9], or combined approaches [10,11]. The removal methods, including soaking in acid, thermal, mechanical methods, and using microwaves, are effective for reducing the amount of residual mortar; however, these methods pose serious risks to the environment and human safety [12–14]. Methods to improve the bond strength of the adhered mortar include chemical techniques such as polymer impregnation, pozzolanic coatings, accelerated carbonation curing, spraying, and bio-deposition. Chemical techniques are considered more sustainable methods for reducing the porosity of RCA and improving the interfacial transition zone (ITZ). Some chemical techniques have shown promise for providing a great level of improvement, such as spraying [8], and soaking with silica fume [15]. Amongst the various studies, there is inconsistency in the degree of improvement in the mechanical and durability properties of RAC that has been subjected to pretreatment of RCA. Certain pretreatment methods cannot be used in practice. Specific techniques, such as CO_2 curing and bio-deposition, require specialized equipment and controlled conditions [16,17]. Other methods, such as soaking in strongly acidic solutions, result in hazardous waste and present environmental concerns [18].

For many of today's challenges, including predicting RAC strength, Machine Learning (ML), both supervised and unsupervised, has, to date, been more accurate than traditional regression methods (linear and nonlinear). Unlike traditional empirical or semi-empirical models that impose rigid functional forms, ML can leverage complex, nonlinear relationships in experimental data [19,20]. As with most empirical models, ML can incorporate multiple interactive or dependent factors that influence RAC properties (RCA content, curing age, curing method, and replacement ratio) in ways that traditional models do not account for effectively. In addition, ML has grown due to the availability of Open Datasets and transfer-less Algorithms, as well as Free and Open-Source Software (FOSS) Libraries that require less lab testing; therefore, ML represents a scalable, economical, and resource-efficient option for predicting the compressive strength of RAC [21].

The production of concrete generates significant carbon emissions and consumes a significant amount of energy. The ever-increasing demand for concrete continues to exert pressure on the Earth's natural resources and raises concerns about both environmental sustainability and human health. As a result, this situation promotes the search for alternative materials that can reduce the environmental effects of concrete while maintaining the required engineering performance. One common alternative is replacing natural aggregate with RCA. Many life cycle assessment (LCA) studies have evaluated the sustainability of concrete with RCA; the reported RCA replacement levels typically range from 10% to 100%, and the compressive strengths of the mixtures can be extremely different from one another [22–25]. A number of these studies compared and contrasted different compositions of RAC with conventional concrete produced with virgin natural aggregate, noting that the environmental impact associated with producing concrete with RCA primarily depends on the replacement ratio, the distance transported, and the processing requirements of the RCA [26,27]. In addition, concrete systems that combine RCA with supplementary cementitious materials have also been investigated; the results of these studies indicate that the environmental impacts of such systems tend to be lower than those of systems that use only RCA [23,28,29].

Research has examined the impact of various replacement ratios of RCA and treatment methods; however, very few studies have investigated practical, scalable treatments that can be implemented in real-world settings and are eco-friendly (without hard waste). Additionally, although many ML models have been developed to evaluate how well concrete will perform in terms of compressive strength, most use established Concrete Mix Designs and only provide input data for untreated RCA. There is a lack of research specifically relating the mechanical properties of sustainable concrete made from treated recycled concrete aggregates to a complete LCA. This study addresses the gaps by experimentally testing an additional set of hybrid RCA treatments: RCA 1: acetic acid soaking combined with silica fume spraying; RCA 2: sodium silicate spraying followed by silica fume; RCA 3: acetic acid soaking, sodium silicate spraying, and silica fume application.

In comparison with other conventional methods of treating RCA, the proposed hybrid method has many technical, economic, and environmental advantages.

1. Controlled Acid Treatment

The RCA was treated with 5% acetic acid solution to remove loosely bound mortar. Acetic acid is less aggressive than other acids used in the treatment of aggregates. Acetic acid does not introduce deleterious ionic species in the form of chlorides or sulphates.

2. Reduced Chemical Consumption

The application of sodium silicate and silica fume was done through spraying, which reduced the consumption of these chemicals. The spraying method ensures that only the required amount of chemical is used in the treatment of aggregates.

3. Reduced Environmental Impact

The spraying method does not require large volumes of chemicals, which in turn reduces wastewater generation. The use of acetic acid also reduces the ionic contaminants.

4. Enhanced Surface Characteristics

The acid treatment of aggregates provides a cleaner surface. The application of sodium silicate and silica fume also increases the density of the surface.

5. Economical and Feasible

The procedure does not require complex equipment and can be scaled for practical application.

Furthermore, this study builds a predictive ML model using both treated and untreated RCA data across a variety of natural coarse aggregate (NA) replacement ratios and Pozzolanic Reactivity Levels. SHAP Analysis helps to assess the impact of each input variable on compressive strength, increasing interpretability. Web-based dashboard functionality provides real-time opportunities for Researchers and Practitioners to support Sustainable Concrete Design. By integrating innovative RCA treatment technologies with ML-based predictive capabilities, this research enables the large-scale adoption of high-performance recycled concrete. Finally, an LCA was performed to determine the embodied carbon from the analyzed concrete mixes and assess the potential environmental impacts between systems. An economic assessment was also completed to determine the viability of utilizing the proposed RCA treatment options.

2. Review of ML Models for Compressive Strengths of Recycled Aggregate Concrete

Recent studies have also applied a variety of ML models to predict compressive strength, as listed in Table 1. The initial studies on RAC's compressive strength prediction focused on classical regression and tree-based models. For example, [21] considered linear and nonlinear regression, an artificial neural network (ANN), a random forest (RF), and M5P on a database containing 90 instances with an 80:20 training–test split, and reported that RF was the best predictor. The increased number of instances enabled the application of ensemble models, which gained prominence in recent studies on RAC's compressive strength prediction. For example, study [30], which considered a database containing 638 instances, reported that RF was the best predictor of compressive and flexural strength across both train–test splits and k-fold cross-validation. More comprehensive comparisons were also conducted across a variety of machine learning models for predicting compressive strength, including ANN, SVR, DT, RF, KNN, AdaBoost, Bagging, XGBoost, and CatBoost, with CatBoost reported as the top predictor by the study [31]. In addition, study [32] also considered a database containing 521 instances, comparing RF, SVR, KNN, XGBoost, and GBDT, with GBDT being reported as the top predictor among the considered models. Some studies also focused on cross-validation strategies. For instance, study [33] performed 10-fold cross-validation on 962 data samples, and GB was reported as the top-performing model. Study [34] produced a top-performing model. More recent studies have also started employing boosting-based algorithms. For instance, study [35] compared RF, ERT, GB, LGBM, XGB, CB, and other models on a 70–30 split, and reported that RF and GB were the top-performing models. Study [36] adopted a 70–15–15 split, and Extra Trees and KNN were reported as the top-performing models. Study [37] also adopted internal and external validation, and RF and XGB were reported as top-performing models with regard to predictive accuracy. Ensemble-based models, including RF, GB, ET, and XGB, have been reported to display high predictive potential across many studies. However, many studies have adopted a simple train–test split, and some studies have also adopted limited hyperparameter tuning. Therefore, this study adopted Bayesian hyperparameter optimization with Optuna 4.8.0, along with k-fold cross-validation on the training set, followed by a test evaluation approach.

Table 1. Summary of ML models for concrete compressive strength prediction.

Study	ML Models	Dataset	Validation Method	Best Model	Output/Target
[38]	Linear, nonlinear regression, RF, ANN, M5P	90	80–20 simple train–test split	Random Forest	Compressive strength
[30]	RF, Gradient Boosting	638	80–20 train–test split, k-fold cross-validation	Random Forest	Compressive & flexural strength
[31]	ANN, SVR, DT, RF, K-NN, AdaBoost, Bagging, XGBoost, CatBoost	-	-	CatBoost	Compressive strength
[32]	RF, SVR, KNN, XGBoost, GBDT	521	train–test split and k-fold cross-	GBDT	Compressive strength
[33]	RF, GB, AB, KNN, BR, SV, XGB, DT, ANN, and	962	10-fold cross-validation.	GB	Compressive strength
[34]	MPR, LR, and SVM	125	80–20 train–test split and 5 k-fold cross-validation	MPR	Compressive strength
[35]	RF, KNN, ERT, GB, LGBM, XGB, CB, GAM1, and GAM2	515	70–30 train–test split	RF, GB	Compressive strength
[36]	XG, Boosting, Ada Boosting, ET, DT, RF, SVM, GB, KNN, CB	515	70–15–15 train–validation–test split	ET, KNN	Compressive strength
[37]	LR, DT, ANN, RF, and XGB	744	Internal & External	RF, XGB	Compressive strength

Linear regression (LR), Random Forest (RF), decision tree (DT), artificial neural network (ANN), XGBoost (XGB), Gradient Boosting (GB), M5P model (M5P), Support Vector Regression (SVR), K-Nearest Neighbors (KNN), CatBoost (CB), Extra Trees (ERT), AdaBoost (AB), Light GB, Categorical Gradient Boost (CGB), Hist Gradient Boosting (HGB), Gradient Boosting decision tree (GBDT), multiple nonlinear regression (MPR), Inverse Gaussian (GAM1) and Poisson (GAM2).

The models selected in this study formed an ensemble; all were tree-based and were chosen because they were well-suited to modeling the complex behaviors of RCA concrete. Many variables influence the compressive strength of RAC, including mix proportions, curing conditions, surface treatments, and the presence of adhered mortar creates variability, as does the heterogeneous nature of the RCA. The effect of all these factors results in many nonlinear and coupled relationships, which are difficult to capture with traditional regression models; therefore, tree-based methods provide the best solution for handling this level of complexity. Furthermore, tree-based ensemble methods can effectively model nonlinear interactions and manage heterogeneous datasets, while being resilient to errors in the response variable and different levels of variable importance.

3. Experimental Program

3.1. Material

3.1.1. Pozzolanic Material

In all mixes, Ordinary Portland Cement (OPC) complying with EN 197-1 (CEM I) [39] was used as the primary binder. In addition, supplementary pozzolanic materials have been added to partially replace cement, improve performance, and treat the material. Silica fume was provided by Master Builders (Manchester, UK) for research purposes (MasterRoc MS 610) and complied with all requirements stated in EN 13263-1 [40] requirements for Class 1 silica fume. The properties of these materials, as specified by the supplier and in compliance with standards, are outlined in Table 2.

Table 2. Chemical composition of various cementitious materials.

Oxide/Component	Type I Cement	Silica Fume
SiO_2	20.1%	94%
Al_2O_3	4.6%	0.5%
Fe_2O_3	2.0%	1.5%
CaO	65.1%	0.8%
MgO	4.5%	0.1%
K_2O	—	1%
Na_2O	—	0.2%
TiO_2	—	—
MnO	—	—
S^{2-}/SO_3	2.8% (SO_3)	—
Cl^-	—	<0.1%
L.O.I.	1.4%	—

3.1.2. Aggregate

The fine aggregate consists of natural sand; the size of the aggregate does not exceed 2.36 mm. The fine aggregate was dried in an oven to remove any moisture. The NA used in this study was crushed stone obtained from a local supplier, Travis Perkins. The maximum aggregate size was 20 mm, as in the RCA. The RCA obtained from waste concrete cubes with compressive strengths ranging from 25 to 45 MPa was collected and crushed in the laboratory. The resulting material was classified as recycled aggregate, as shown in Figure 2. The maximum RCA size was 20 mm. The particle-size distribution of the aggregate is shown in Figure 3.

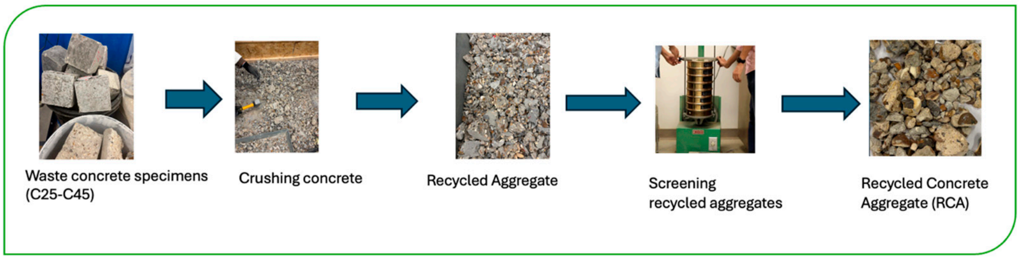

Figure 2. Preparation of Recycled Coarse Aggregate (RCA).

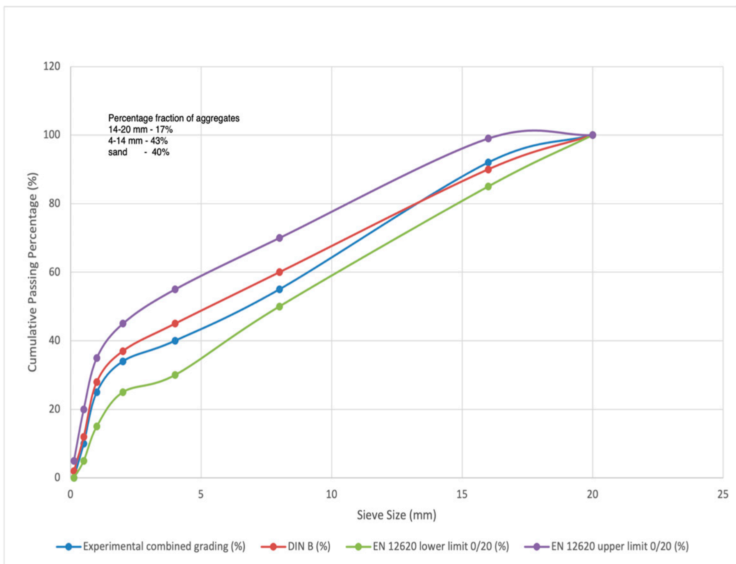

Figure 3. The distribution of particle sizes [41].

3.1.3. Acetic Acid

For this study, Acetic Acid 77%, supplied by Valet Chem (Tockwith, UK), was used. This high-concentration, industrial-grade acetic acid solution was diluted with water to achieve a 5% concentration.

3.1.4. Water and Superplasticizer

Tap water was used for concrete mixtures. This study used Sika Viscocrete-10 (GB) as an admixture, a high-range water reducer, and met the requirements of BS EN 934-2 to enhance the workability of the concrete mix and the performance.

3.1.5. Liquid Sodium Silicate

Liquid sodium silicate, also known as water glass or liquid glass, was used in this study. The sodium silicate solution used in this study had a concentration of 40% and a density of 1.41 g/cm^3.

3.2. Treatment Method

3.2.1. First Treatment (RCA1)

RCA was subjected to a hybrid treatment process to enhance its quality. The first step was soaking in a plastic container containing acetic acid. The effectiveness of acetic acid treatment for improving the quality of RCA depends on several factors, including acetic acid concentration and immersion time. Recent studies [12,42,43] have shown that applying a 5% acetic acid solution for 3 days enhances the overall properties of RCA. After soaking, the RA was left to dry in the open air for 2 days; this treatment aimed to improve the RCA's quality by reducing porosity and enhancing its properties. In the second phase, the treated RCA was placed in a tray and vibrated. A 5% silica fume solution (by weight of the RCA) was prepared by mixing silica fume with water. The solution was sprayed onto the RCA while the tray was vibrating, ensuring uniform coverage of all particles. The treated RCA (RCA1) was allowed to dry for 24 h, thereby promoting bonding between the silica fume and the RCA and improving its surface properties (Figure 4a). Acidic treatment helps remove old, adhered mortar and partially dissolves the calcium hydroxide ($Ca(OH)_2$) to create a rough, chemically reactive surface, which increases the number of reactive sites available. The silica fume that is applied also fills some of the surface pore spaces and reacts pozzolanically with any remaining $Ca(OH)_2$ to produce more calcium silicate hydrate (C-S-H) gel. This combination of effects increases the bonding between the interfacial boundaries while reducing the porosity of the treated RCA, resulting in the improved performance of the treated RCA.

(**a**)

Figure 4. *Cont.*

(**b**)

(**c**)

Figure 4. RCA after treatment: (**a**) RCA1, (**b**) RCA2, (**c**) RCA3.

3.2.2. Second Treatment (RCA2)

The second treatment, RCA, was sprayed with a 40% sodium silicate solution. After the sodium silicate was added, the mixture was held for 30 min to allow the bond to form. The RCA was then sprayed with the silica fume solution, and the same procedure was conducted as in the first treatment. The treated aggregate obtained from this process was designated as RCA2 (Figure 4b).

3.2.3. Third Treatment (RCA3)

The RCA underwent a three-step procedure: it was treated in a 5% acetic acid solution for 3 days, and then air-dried for 48 h after removal from the acid bath. The second step involved spraying the prepared RCA with a 40% sodium silicate solution and air-drying it for 30 min to allow the sodium silicate to bond chemically to the aggregate surface.

In the final step, the prepared RCA was placed in a vibrating tray and sprayed with a silica fume solution containing 5% by weight of the RCA. Finally, in the third treatment procedure, the treated RA was air-dried for 24 h, yielding RCA3 with improved surface properties due to the cross-linking action of the sodium silicate and silica fume solutions, thereby reducing the pore volume (Figure 4c).

3.3. Proportioning of Materials

The water-to-cement ratio of each concrete mixture was 0.47, and the effective water content was 180 kg/m^3. The cement content was constant at 386 kg/m^3, and natural sand was included at 756 kg/m^3 in each combination. RCA was included at 1020 kg/m^3 in each RAC combination with zero natural coarse aggregate. A control mixture of NAC was utilized as a reference. The amounts of desired water added varied across combinations to compensate for water absorption from recycled aggregate. In the RAC+SF mixture, silica fume was added at 5% by weight of RCA. This percentage was selected because it was equal to the amount of silica fume used in the pretreatment of RCA in the mixtures tested (RAC1, RAC2, and RAC3). The reason for a direct comparison of adding silica fume to the concrete mixture compared to applying silica fume as a surface treatment to the RCA is to help clarify whether the improvement in performance is due to the presence of silica fume itself or its impact on changing the surface characteristics of the recycled aggregate. The need for additional water increased for untreated recycled aggregate mixtures and decreased for pre-sprayed mixtures (RAC1, RAC2, and RAC3) as a result of the treatment. A superplasticizer was used in all combinations at 1% by weight of cement in all combinations. The features of the mix design are shown in Table 3.

Table 3. Mix proportions of the concrete mixtures.

Concrete Label	W/C Ratio	Effective Water (kg/m^3)	Additional Water (kg/m^3)	Cement (kg/m^3)	Sand (kg/m^3)	RCA (kg/m^3)	NA (kg/m^3)	SF/RCA Ratio%	SP
NAC	0.47	180	0	386	756	0	1020	0	1
RAC control	0.47	180	50.4	386	756	1020	0	0	1
RAC+SF	0.47	180	52.7	386	756	1020	0	5	1
RAC1	0.47	180	11.4	386	756	1020	0	0	1
RAC2	0.47	180	13.7	386	756	1020	0	0	1
RAC3	0.47	180	7.6	386	756	1020	0	0	1

3.4. Testing Methods

3.4.1. Physical Properties Test

The physical properties of normal aggregates and RCA were examined for water absorption, density, and bulk density, in accordance with EN 1097-6 and EN 1097-3, respectively. For RCA, representative samples were obtained by thoroughly mixing and quartering to account for variability in the amount of adhered mortar across particles.

3.4.2. Evaluation of Adhered Mortar Removal from RCA Using 5% Acetic Acid

To determine the mortar loss from the RCA, the coarse aggregate was sieved, and the aggregate passing the sieve with an opening size of 4.75–20 mm was collected. The collected sample was put in an oven at 100 ± 5 °C for 24 h. The weight of the dried sample was noted as the initial mass (W1). The sample was then transferred into a plastic container. The 5% acetic acid solution was prepared, and 2 L of the solution was transferred into the container so that the RCA could be fully immersed. Then, the RCA sample was left in the acetic acid solution for 3 days at room temperature. After the required time, the sample was removed, and the acetic acid-treated sample was then dried in an oven at 100 ± 5 °C for 24 h. The sample was then left at 25 ± 1 °C for 24 h. The sample was then sieved using a 4.75 mm sieve to maintain the aggregate size between 5 and 20 mm. The sample was then weighed and recorded as the final mass (W2).

The mortar loss from the sample was calculated using the formula:

$$\text{Mortar loss (\%)} = (W1 - W2)/W1 \times 100 \tag{1}$$

3.4.3. Experimental Slump Test

The slump test was performed according to the procedures specified in BS EN 12350-2:2009 [44]. The S2 class's target slump range was 50–90 mm. As soon as the concrete was mixed, samples were tested to assess workability.

https://doi.org/10.3390/su18073541

3.4.4. Moisture Content (%) Test

Moisture amount is a key indicator of concrete's porosity and durability. The concrete samples were first dipped in water for 24 h. After this, the samples were removed from the water tank and dried with a towel to remove the free water. The specimens were then weighed to obtain their saturated weights. The specimens were then placed in an oven at 105 °C for 24 h, after which they were weighed again to obtain their dry weights. The difference in weights was then used to obtain the moisture content.

3.4.5. Compressive Strength Testing of Concrete Specimens

The compressive strength of concrete samples was measured at 28 and 90 days following BS EN 12390-3 [45]. For each concrete mixture, three cube specimens (100 mm × 100 mm × 100 mm) were tested. Loading was performed in uniaxial compression at a constant rate of 6 kN/s.

4. Machine Learning Models

4.1. ML Workflow for RCA Treatment Prediction

Using literature and experimental data to train an ML model required that the raw data be cleansed, encoded, and scaled for consistency. Various regression models were evaluated, and SHAP analysis was used to assess feature influence; an interface was developed for everyday use. The ML process presented in this project is shown in Figure 5 below.

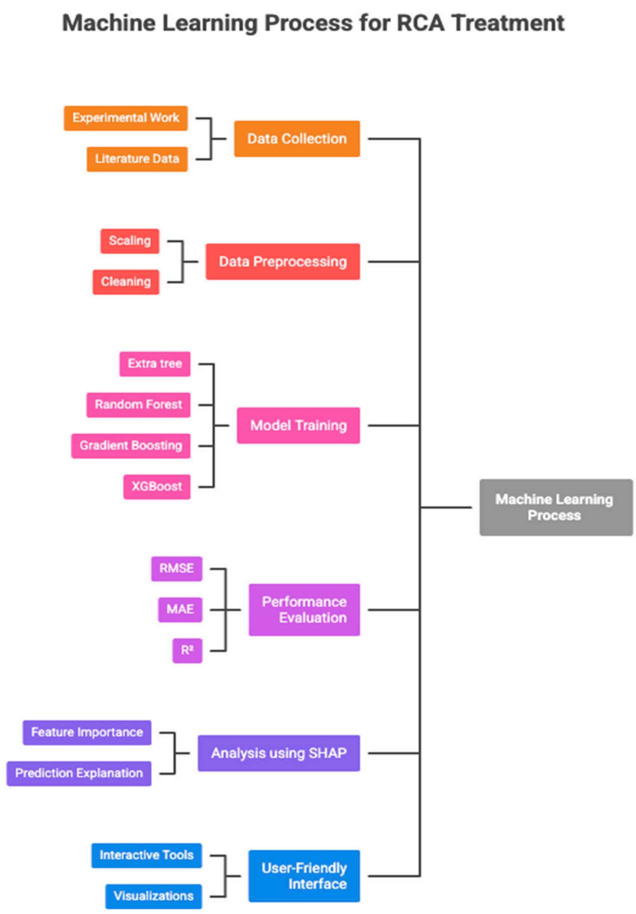

Figure 5. Flowchart of the ML process.

4.2. Concrete Database Collection

This study presents a composite dataset comprising 478 data points for use by training models to predict concrete compressive strength. This dataset contains experimental results from this research, as well as additional data collected from 21 different peer-reviewed journal articles [7–9,11,12,42,46–60]. Each data point in the dataset represents a complete description of the concrete mixture design; therefore, it provides information on the amounts of the different materials used: fine aggregate, water, cement, natural coarse aggregate, and RCA. Mineral additives such as ground granulated blast-furnace slag (GGBS), fly ash, and silica fume, as well as chemical admixtures such as superplasticizers, are also identified in the dataset. In addition to providing a description of the concrete mixture, the dataset identifies the RCA replacement ratio, the water-to-cement ratio, and the curing age (in days) for each concrete mixture. To understand the effect of improving the compressive strength of a concrete mixture through the use of various methods, the dataset also includes descriptors for enhancement technique parameters such as acid soaking (acetic acid and hydrochloric acid (HCl)), numerical value of soaking duration in days, spraying treatments (sodium silicate, silica fume, nano silica), length of mechanical treatment and materials pre-soaking the concrete mixture (sodium silicate, fly ash, silica fume, and cement). The dosages and quantities of cementitious material and aggregate used in each concrete mixture are expressed in kilograms per cubic meter (kg/m^3), whereas the target output for the dataset is the concrete mixtures' compressive strength (MPa). Descriptive statistics and variable names for the dataset are given in Table 4.

Table 4. Distribution properties of input and output parameters.

Variable	Unit	STDEV	Max	Min	Average
Cement	kg/m^3	109.86	539	78	409.19
Fly ash		32.91	127	0	9.25
Silica fume		10.86	56	0	4.07
GGBS		13.62	78	0	4.44
Natural coarse aggregate		317.08	1003	0	283.62
Recycled coarse aggregate		376.33	1330	138	745.12
Fine aggregate		117.9	1192	384.8	692.29
Water		37.01	282.2	96	193.36
Superplasticizer	%	0.61	2	0	0.42
Curing duration	Days	29.87	180	1	29.67
Sprinkling (silica fume, nano silica)/RCA ratio	%	1.69	8	1	4.71
Acid soaking (acetic, HCL)		1.76	10	0.37	2.56
Duration of mechanical treatment	min	4.03	12	1	5.73
Spraying sodium silicate concentration	%	11.55	60	20	40
Pre-soaking (cement, metakaolin, silica fume, fly ash)	%	19.41	66.7	7	19.8
Pre-soaking sodium silicate concentration		16.75	45	3	19.26
Compressive strength	MPa	12.52	115.27	15	40

4.3. Model Training

A structured machine learning framework was adopted to ensure effective model development and fair performance assessment. The data was split into a training set (80%) and a test set (20%). The training set was used to develop the models, while the test set was held back for the final assessment. The hyperparameter tuning was performed using the Optuna library, which uses Bayesian optimization. Unlike the grid search technique, the Bayesian optimization technique is more efficient, especially for complex problems, since it searches the hyperparameter space adaptively, learning from the results of the trials to concentrate the search in promising regions. For each model, the key hyperparameters include the number of estimators, tree depth, learning rate, subsampling ratio, and feature sampling ratio. To ensure an accurate estimate of the model's performance during the hyperparameter optimization, 10-fold cross-validation was adopted on the training data. The data in the training set was split into 10 sets, and the model was trained on 9 sets and validated on the remaining 1. The model was selected because it had the best predictive performance. Table 5 presents the details. Four ML models were evaluated to develop a robust and accurate predictive model for the compressive strength of RCA-treated material, as discussed below.

Table 5. Comparison of four models with their top hyperparameters.

Model	Hyperparameter	Range	Best Value
Random Forest Regression (RF)	n_estimators	[50, 1000]	387
	max_depth	[10, 50]	15
	min_samples_split	[2, 10]	4
	min_samples_leaf	[1, 40]	1
Extra Trees Regressor (ET)	n_estimators	[10, 1000]	115
	max_depth	[3, 50]	33
	min_samples_split	[2, 10]	3
	min_samples_leaf	[1, 40]	1
Gradient Boosting (GB)	n_estimators	[50, 1000]	813
	learning_rate	[0.02, 0.5]	0.1059867
	max_depth	[2, 8]	2
	min_samples_split	[2, 6]	3
	min_samples_leaf	[1, 40]	2
XGBoost (XGB)	n_estimators	[50, 1000]	953
	learning_rate	[0.01, 0.3]	0.1364264
	max_depth	[2, 10]	4
	subsample	[0.5, 1]	0.9476815
	colsample_bytree	[0.5, 1]	0.8047659

4.3.1. Random Forest

Random Forest (RF) is an ensemble method that improves predictive performance by combining multiple decision trees. Each decision tree is trained using a bootstrapped training set and random parameter selection, collectively referred to as bootstrapped aggregation (bagging). By incorporating diversity among trees, RF can be made a more stable model while minimizing overfitting [61]. A recent study by [30] used RF to predict the compressive strength of RAC and showed better performance than single-decision-tree models.

4.3.2. Extreme Gradient Boosting (XGBoost)

It is a sequential learning algorithm that builds decision trees, with each new tree correcting the errors of prior trees. By modelling only the residuals, this model corrects its errors and achieves good predictive performance with high accuracy. The boost-like method of construction is well suited to solving complex nonlinear problems. XGBoost 3.2.0 has been used in novel predictive frameworks for RCA-based concrete [62].

4.3.3. Gradient Boosting (GB)

It is an iterative ensemble model that provides strong predictive performance by combining the additive predictions of many weak learners, typically decision trees. In each iteration, a tree is learned to fix the residuals from the previous ensemble and minimize a given loss function. The process is continuous until the model can be thought of as "converging" towards an optimal solution. GB is particularly useful at taking complex patterns and improving prediction accuracy at each step [63].

4.3.4. Extra Trees (ET)

ET is an extension of the Random Forest method. The difference is that it improves accuracy by constructing a more diverse ensemble of decision trees. It achieves this by introducing greater randomness: instead of selecting feature subsets and split points semi-randomly, ET selects them at a fully random level at each node. As a result, you obtain a broader array of trees, and the final prediction is the average across the trees in the ensemble. ET is also robust to noise and irrelevant features, thus providing stable and strong performance on complex regression tasks [64].

4.4. Model Evaluation

To predict the compressive strength of RAC, this paper has assessed four ML models. Results from the models were compared using various statistical measures, including root mean square error (RMSE), mean absolute error (MAE), the coefficient of determination (R^2), and the Pearson correlation coefficient between measured and predicted values. The formulas for the three metrics can be found in the following equations:

$$\mathrm{MAE} = (1/\mathrm{n})\sum_{i=1}^{n}|y_{\mathrm{i}} - \hat{y}_{\mathrm{i}}| \tag{2}$$

$$\mathrm{RMSE} = \sqrt{\frac{1}{n}\sum_{i-1}^{n}(y_{\mathrm{i}} - \hat{y}_{\mathrm{i}})^2} \tag{3}$$

$$\mathrm{R}^2 = 1 - \frac{\sum_{i-1}^{n}(y_{\mathrm{i}} - \hat{y}_{\mathrm{i}})^2}{\sum_{i-1}^{n}(y_{\mathrm{i}} - y)^2} \tag{4}$$

where y_{i} is the observed compressive strength, $\hat{y}_{\mathrm{i}}$ is the predicted compressive strength, y is the mean of observed values, and n is the number of samples. These metrics present individual prediction performance and the model's overall fit across the entire dataset. MAE and RMSE denote the average deviation of predictions, whereas R^2 and correlation metrics quantify the strength and consistency of the predictions. These metrics would enable a quantitative comparison of predictive reliability across models, their sensitivities to input variability, and their generalization to unseen data.

4.5. Shapley Additive Explanations (SHAP)

It is a unified framework for interpreting machine learning models by allocating a contribution value (SHAP value) to each feature for a particular prediction. SHAP is grounded in Shapley values in cooperative game theory, which fairly allocates the "credit" or "blame" among features by considering every combination of features. It models the prediction as the sum of each feature's contribution, so interpretation is very natural and consistent. A positive SHAP value shows that the feature increases the prediction; a negative SHAP value shows that the feature decreases the prediction. This makes it a beneficial and resourceful explanatory framework grounded in mathematics; it provides a transparent way to explain complex models in a mathematically rigorous manner, as in Shapley, which has been well received by the scientific community [65].

4.6. User-Friendly Interface

Gradio 5.50.0 provides a user-friendly interface for building applications in a few lines of code and deploys them online via Hugging Face. Once the ML models are tested, the model that performs best will be selected, as it has proven to be the most accurate in the task of

https://doi.org/10.3390/su18073541

prediction. The selected model will predict the strength of RAC after several types of treatment, and the interaction will occur via the Gradio user interface for easy, accurate predictions.

5. Environmental Impact Aspect

When determining whether RCA production and consumption are sustainable, the environmental impact of both must be considered. Therefore, the purpose of this research is to evaluate various types of surface-treated RCA by examining, through LCA, the environmental benefits of replacing natural aggregate with RCA. In order to evaluate the cost of treated RCA from an economic point of view, economic analysis will be conducted to compare the cost of treatment and material reuse versus the cost of sustainable materials.

5.1. Goal and Scope

This study quantified the carbon footprint associated with low-carbon concrete made with RCA. LCA was conducted to evaluate the environmental performance of treated RCA. The analysis includes the various processes throughout the life of recycled aggregate concrete that contribute to environmental impact. These processes include the extraction of raw materials, transportation, treatment, and manufacturing of concrete. The LCA conducted in this study was performed in accordance with the International Organization for Standardization (ISO), which provides the methodological framework for conducting an LCA. The ISO standard for LCA specifically outlines how to conduct a life cycle assessment of a product [28,66]. The initial phase of the project is to conduct a Life Cycle Inventory (LCI). In this state, the relevant data pertaining to the input of materials, the consumption of resources, and emissions into the environment for the product system is collected. Data should also include quantities of all materials consumed and their embodied carbon values. Once the LCI is performed, a Life Cycle Impact Assessment (LCIA) calculates the environmental impacts for each input and emission source. The last part of the process is called life cycle interpretation. In this step of the analysis, the results of the LCI and LCIA are interpreted to identify the primary sources of carbon emissions in concrete production, as well as develop recommendations to reduce the embodied carbon content of concrete in the construction industry [67,68].

5.2. Life Cycle Inventory

This study compiled the Life Cycle Inventory (LCI) from a variety of sources, including experimental results and the literature. The amount of materials used to create each concrete mix was obtained from testing done in the laboratory, while the embodied carbon for the cement, aggregate, water, and superplasticizer was taken from the Inventory of Carbon (ICE v3.0) [69] Emissions values for acetic acid, sodium silicate, and silica fume were obtained from the recent literature and industrial suppliers to ensure global representativeness. All these results were normalized to a functional unit of 1 cubic meter of concrete to facilitate direct comparison of the different mix designs. A summary of the embodied carbon contributions of all the materials is contained in Table 6, which includes those associated with treatment.

Table 6. Summary of embodied carbon intensity for study materials.

Ingredient	Embodied Carbon Factor (kg CO_2 e/kg)
Portland Cement	0.91
Fine Aggregates (Sand)	0.005
(NCA)	0.005
(RCA)	0.002
Water	0.00034
Superplasticizer	2.4

Table 6. *Cont.*

Ingredient	Embodied Carbon Factor (kg CO_2 e/kg)
Acetic Acid	1.7
Sodium Silicate	0.5
Silica Fume	0.02

5.3. Life Cycle Impact Assessment (LCIA)

To calculate the environmental impact for each concrete mix, the life cycle assessment measured the amount of embodied carbon, or CO_2-equivalent in KG, associated with each mix. The study used one cubic meter as a functional unit for developing the environmental performance of the various types of concrete mixtures.

The life cycle assessment was cradle to gate, A1, A2, and A3, as defined in ISO 14044 [70], which allows for the evaluation of the environmental impact of each concrete mix. The life cycle of a concrete mixture has three phases: The A1 portion (raw material stage) includes cement manufacture, natural aggregate extraction and processing, recycled aggregate processing, silica fume, and chemical treatments (acetic acid and sodium silicate). A2 and A3 were not explicitly modeled with respect to transport distances and energy consumption. Rather, their contributions to the overall assessment were implicitly included in the embodied carbon emission factors used, derived from ICE, and the other literature sources. As neither the use, maintenance, nor end-of-life phase was evaluated in this assessment, the life cycle assessment focused exclusively on the production phase, as the production phase is where most embodied carbon emissions are generated. To calculate embodied carbon for materials, use the quantity of each material and multiply it by its respective carbon emission factor. The total embodied carbon for 1 m^3 of concrete is calculated by summing the embodied carbon values of all the materials used. The emission factors used also include any emissions from upstream processes such as production and related transport.

6. Results and Discussion

6.1. Testing Results

6.1.1. Physical Properties of Aggregates

The results for the physical properties of all aggregate varieties are shown in Table 7; all reported values are averages of at least three measurements. The results for the natural aggregate are as follows: density = 2578 kg/m^3, water absorption = 1.9%, bulk density = 1600 kg/m^3. The RCA had greater water absorption and lower density than natural aggregate due to the latent mortar adhering to it. Aggregates treated with RCA1, RCA2, and RCA3 showed improved quality over their untreated counterparts, as evidenced by the fact that RCA1, RCA2, and RCA3 had higher densities and lower water absorption than the untreated RCA, indicating an increase in quality from pretreatment. The treated RCA had higher bulk densities compared to those of untreated RCA, suggesting that the manufacturer's pretreatment improved the overall quality of the treated RCA to be more comparable to that of natural aggregate.

Table 7. Properties of aggregates.

Material	Density (kg/m^3)	Water Absorption (%)	Bulk Density (kg/m^3)
NA	2578	1.9	1600
RCA	2100	8.2	1236
RCA 1	2443	4.73	1503
RCA 2	2388	4.66	1516
RCA 3	2425	5	1401

https://doi.org/10.3390/su18073541

6.1.2. Evaluation of Adhered Mortar Removal from RCA

The mortar loss for the RCA was determined using the acetic acid treatment method. The initial mass before the test (W1) and the final mass (W2) were determined. The mortar loss was calculated to be 1.86%. This low value is related to the use of acetic acid in the treatment process. Acetic acid is a relatively weak acid that removes loosely attached mortar from aggregate particles.

6.1.3. Slump Test Result

The slump results for all samples tested are shown in Figure 6. The NAC slump was 70 mm, and the RAC control had a lower slump due to the high-water absorption rate of the untreated RCA (60 mm). However, by adding silica fume at the same rate as in the other mixes (RAC+SF), we achieved a slump of 65 mm, which was not quite enough to restore full workability. All treated RCAs exhibited an increase in their respective slumps. Both RAC1 and RAC2 achieved slumps of 70 mm, equal to NAC, and the greatest recorded slump occurred with RAC3 (75 mm). This supports the conclusion that treating RCA surfaces provides greater improvement in the workability of fresh concrete than simply adding Silica Fume to the mix.

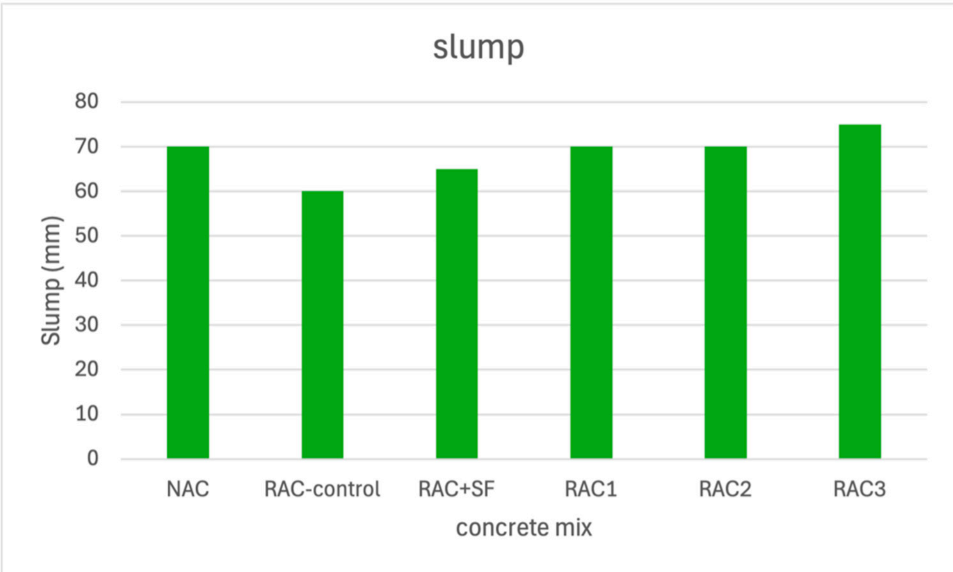

Figure 6. Slump test result.

6.1.4. Moisture Content (%) Result

The results show that the moisture content varies significantly among the concrete mixtures. NAC had the lowest moisture content at 3.49%. This implies that the internal matrix is denser and has lower porosity. However, the RAC mixture had the highest water absorption at 4.86%. This can be attributed to the fact that the recycled aggregates had aged and adhered mortar. Hence, the pore structure is more interconnected. RAC 1 had an intermediate moisture content of 3.99%. However, the water absorption increased again for RAC 2 and RAC 3, recording values of 4.20% and 4.16%, respectively, as shown in Figure 7.

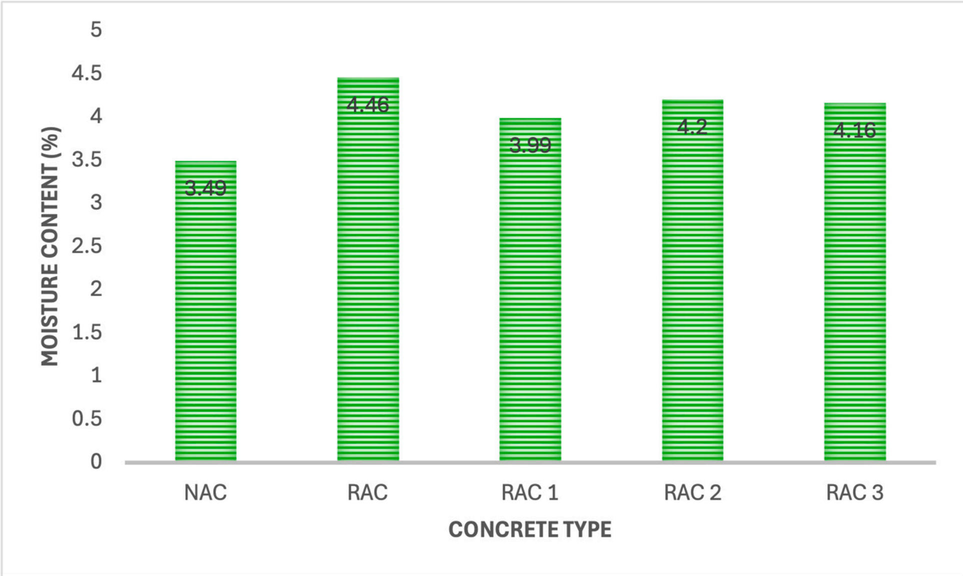

Figure 7. Moisture content results of NAC and RAC concrete mixes.

6.1.5. Compressive Strength

The compressive strength after 28 days and 90 days is shown in Figure 8 for NAC, RAC control, RAC with untreated RCA and silica fume, and RAC with treated RCA (RCA1, RCA2, and RCA3). After 28 days, NAC has a compressive strength of 53.16 MPa, indicating that this is the performance level that sets the benchmark. On the other hand, the RAC control mix has a compressive strength of only 39.42 MPa and thus performs poorly. This indicates that untreated RCA negatively affects compressive strength due to residual old mortar and increased RCA porosity. Using untreated RCA with the same amount of silica fume during the treatment process (RAC+SF) yielded a compressive strength of 46.76 MPa.

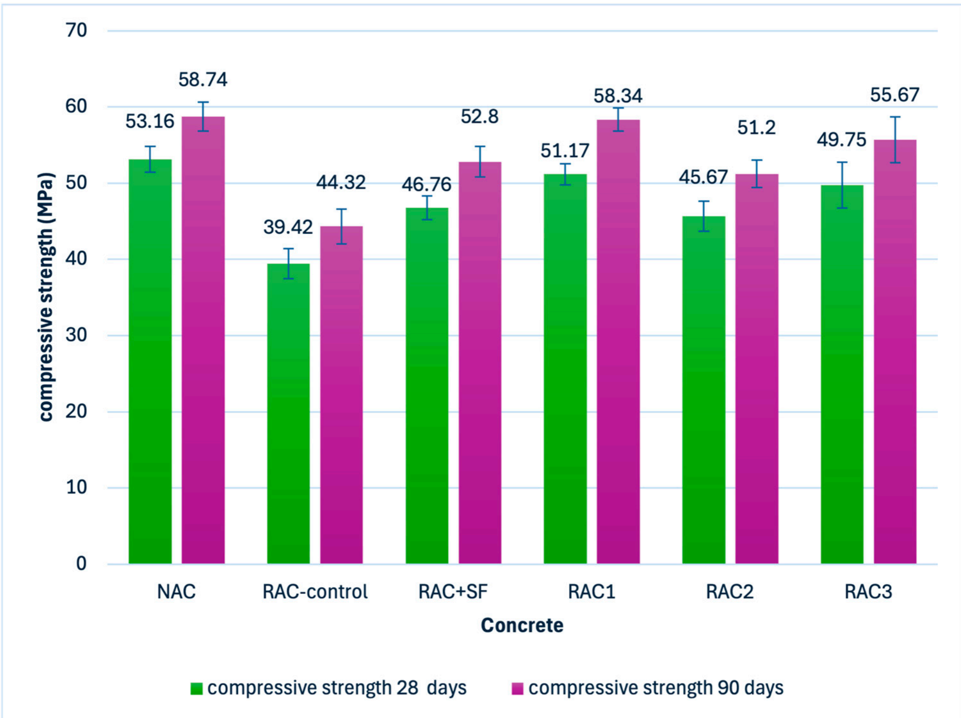

Figure 8. Compressive strength of RAC with different types of treatment.

However, the results of the improvement indicate that although the RCA has been treated with silica fume, the results are still not equivalent to those of NAC; therefore, it can be concluded that the use of silica fume alone, without modification of the RCA surface, does not address the underlying weaknesses inherent in untreated RCA. Using treated RCA also strengthened these mixes. RAC1 had a compressive strength of 51.17 MPa at 28 days, nearly 30% higher than the RAC controls and equal to the NAC strength. This improved strength demonstrates that the combination of acetic acid and silica fume is an effective method for reducing RCA porosity and improving RCA surface quality. The compressive strength of RAC2 was 45.67 MPa, greater than that of the RAC control but less than that of RAC1. The combination of sodium silicate with silica fume improved bonding between cement and RCA; however, without acid pretreatment of the RCA, it was not possible to completely remove poorly adhered mortar from the RCA. The compressive strength of RAC3 at 28 days was 49.75 MPa, slightly lower than that of RAC1. The three-step RCA treatment process continues to improve the RCA surface; however, adding sodium silicate at any step in this series did not provide the early-age strength observed with the RAC1 treatment.

After 90 days, the compressive strength of NAC was recorded as 58.74 MPa, while that of the RAC control was 44.32 MPa. RAC+SF recorded 52.80 MPa, indicating that adding silica fume to cementitious materials can also improve their strength in later hydration phases, though no additional treatment was given to the RCA. The compressive strengths of RAC1, RAC2, and RAC3 were recorded as 58.34 MPa, 51.20 MPa, and 55.67 MPa, respectively. This trend demonstrates that the combination of acid treatment and silica fume spraying was more effective than the intricate multi-step treatment in enhancing compressive strength. The acid treatment reduced the amount of adhering mortar and surface porosity, but the silica fume formed a dense layer that improved the interfacial transition zone and the bonding between aggregate and paste. The results validate that spray-based surface treatment of RCA improves compressive strength. Despite the same amount of silica fume being incorporated into the concrete mix using untreated recycled concrete aggregate (RAC+SF), the resultant strength was inferior to that of mixes using treated recycled concrete aggregate.

6.2. Model Performance

In this study, the performance of four machine learning models was assessed using three evaluation metrics: R^2, RMSE, and MAE. Table 8 highlights the predictive capability of the models on the compressive strength property, both on the training and testing sets. Figure 9 compares the actual values with the model-predicted values.

Table 8. Performance comparison of machine learning models for RAC compressive strength prediction.

Model	Train_R2	Test_R2	Train_RMSE	Test_RMSE	Train_MAE	Test_MAE
RF	0.966	0.873	2.211	5.017	1.448	3.543
GB	0.93	0.883	3.165	4.814	2.366	3.557
XGBoost	0.98	0.909	1.71	4.156	0.81	2.953
ET	0.98	0.905	1.689	4.346	0.679	3.266

The RF model's accuracy on the training dataset was significant, achieving an RMSE of 2.21 MPa, an MAE of 1.45 MPa, and an R^2 of 0.966. On the other hand, the model's accuracy on the test dataset was significant but decreased considerably, achieving an RMSE of 5.02 MPa, an MAE of 3.54 MPa, and an R^2 of 0.87.

It can be noted that GB produced close results across both datasets. As for its results on the training data, it achieved an RMSE of 3.165 MPa, an MAE of 2.366 MPa, and an R^2

https://doi.org/10.3390/su18073541

of 0.93. As for its results on the test data, it achieved an RMSE of 4.814 MPa, an MAE of 3.557 MPa, and an R^2 of 0.883.

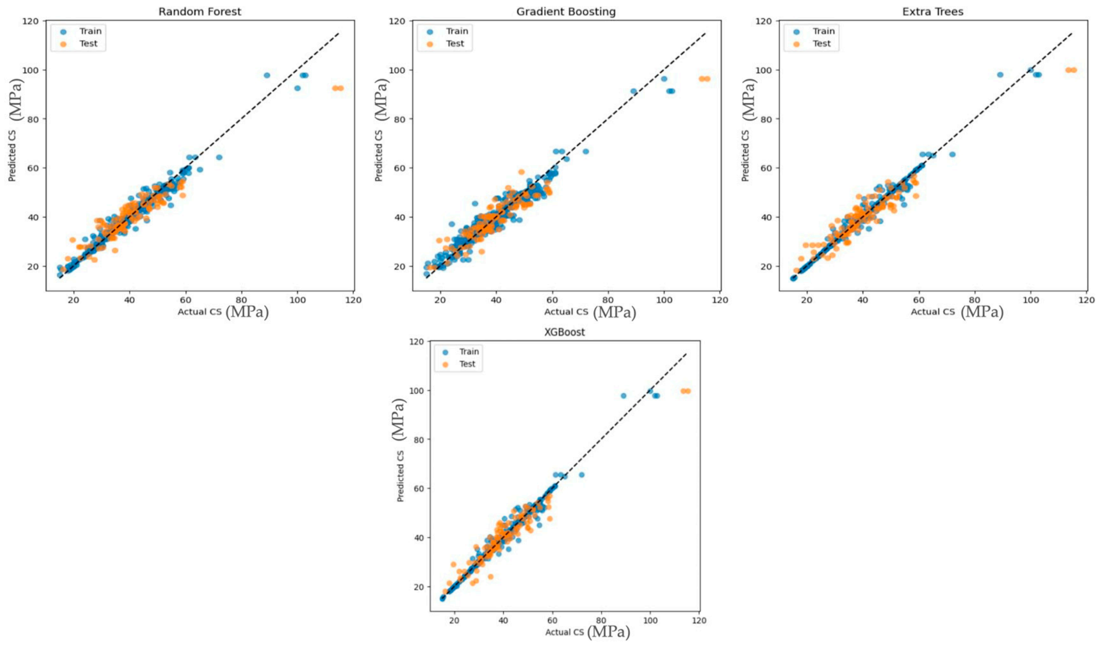

Figure 9. Comparison of actual and predicted compressive strength of RAC.

Higher predictive accuracy was shown by the XGBoost model. On the training data, it had an MAE of 0.81 MPa, an RMSE of 1.71 MPa, and an R^2 of 0.98. With the test data, it had an MAE of 2.953 MPa, an RMSE of 4.156 MPa, and an R^2 of 0.909. From these observations, it is evident that the model is efficient at handling the intricate nonlinear relationships underlying concrete compressive strength.

For the ET model, performance on the training dataset is comparable to XGBoost, with an MAE of 0.679 MPa, an RMSE of 1.689 MPa, and an R^2 of 0.98. On the test dataset, the model had an MAE of 3.266 MPa, an RMSE of 4.346 MPa, and an R^2 of 0.905.

Based on the comparative evaluation of the four models, the final predictive model, XGBoost, was chosen because of its highest test R^2 value, indicating higher accuracy in compressive strength prediction, with fewer errors. Although the Random Forest model showed a larger difference between training and test R^2 values, indicating overfitting, the Extra Trees model also showed good generalization, with test R^2 values similar to those of XGBoost and slightly less variation in error values. XGBoost offers the best reliability in terms of accuracy and consistency of error values.

Figure 10 shows the error histograms, which provide insights into the accuracy of predictions and the generalization ability of the developed models by showing the distribution of errors for both training and test datasets.

For the RF model, it is evident that the distribution of error is centered around zero, which indicates that there is no bias in the predictions of compressive strength. It is also evident that there is a very high degree of fit in the training error, as it is closely clustered around zero. However, in the case of test error, it is evident that there is a wide range of errors, though most of the are still contained within an error band of ±5 MPa.

For the ET model, the errors are tightly clustered around zero in the training data, indicating high accuracy in fitting. For the test data, although the errors are distributed over a wide range, they are still concentrated near zero. This suggests a good generalization ability with no systematic bias in errors and moderate variability.

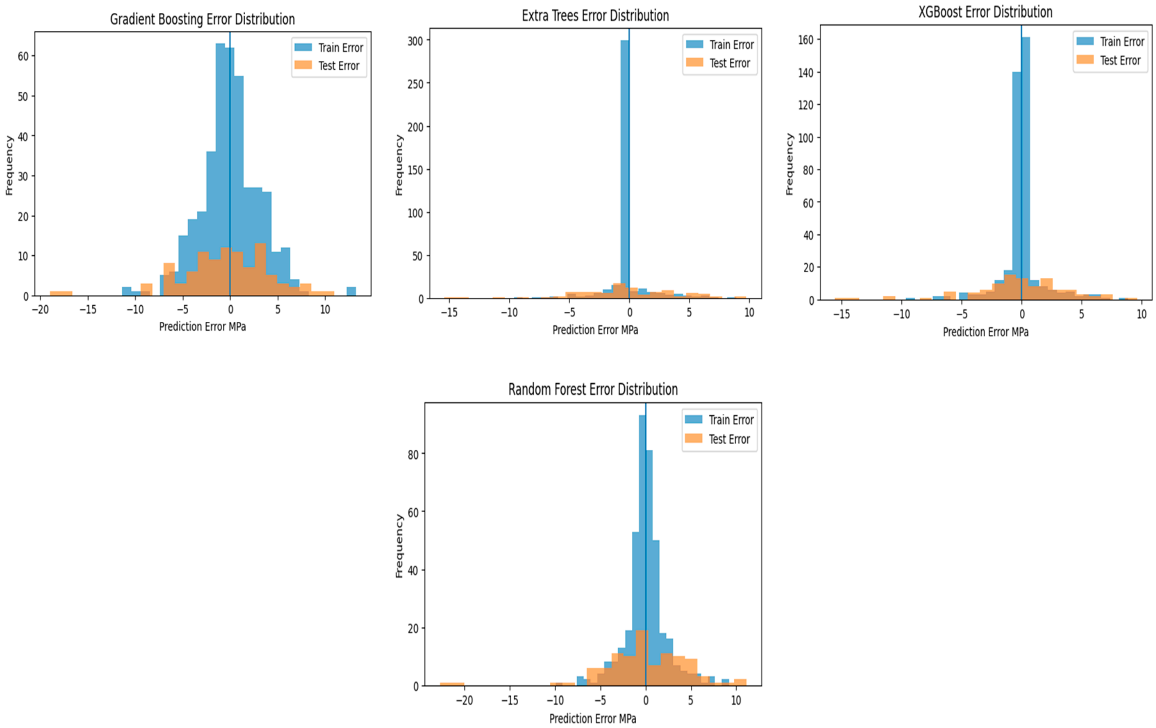

Figure 10. Error distribution of four models for compressive strength prediction. The vertical blue line at zero indicates perfect prediction.

For the GB model, the errors are distributed over a wide range, around ±10 MPa, for both the training and test datasets. However, the peak of errors for the training data is still close to zero, with a much larger variability than in the Extra Trees model. For the test data, it can be noted that the distribution of errors is similar with increased variability, indicating increased prediction uncertainty and a decrease in prediction accuracy.

For the XGBoost model, the errors are sharply concentrated around zero on the training data, indicating high accuracy in fitting. For the test data, the errors are distributed over a wide range, although they remain symmetrical and close to zero.

6.3. Multi-Parameter Interaction Analysis via 3D Response Surfaces

Three-dimensional response surfaces were employed to investigate how RCA treatment conditions interact to influence compressive strength, while keeping all other variables at their mean value. The dataset used in this analysis combines experimental results from this study with data collected from the published literature to expand the range of treatment conditions. The response surfaces demonstrate strong nonlinear interactions between variables, with chemical dosage and treatment time jointly influencing strength, thereby identifying regions of maximum compressive strength, as shown in Figure 11. The interaction between nano silica content and silica fume ratio in the spray treatment creates a distinct high-strength area, where the model predicts a maximum compressive strength of 47.5 MPa. Acid treatments present distinct patterns, where acetic acid treatments present similar compressive strength values at lower concentrations when the soaking time is longer. On the other hand, HCl treatments show sharp increases in predicted compressive strength, suggesting a threshold effect over a short time frame. For slurry treatments, time plays an important role. The silica fume slurry presents a plateau after 75 h of soaking, beyond which additional soaking time provides little additional strength. The cement slurry presents an initial increase in compressive strength followed by a plateau after a minimum soaking time. The sodium silicate slurry presents a strong interaction between concentration and soaking time, where higher concentrations provide additional compressive strength only when soaking times are extended. The combination of spraying sodium silicate percentage and spraying silica fume content presents a coupled effect on compressive strength. Higher predicted strengths are obtained within a specific sodium silicate concentration range when increasing silica fume content, while excessive sodium silicate with low silica fume content provides little additional strength.

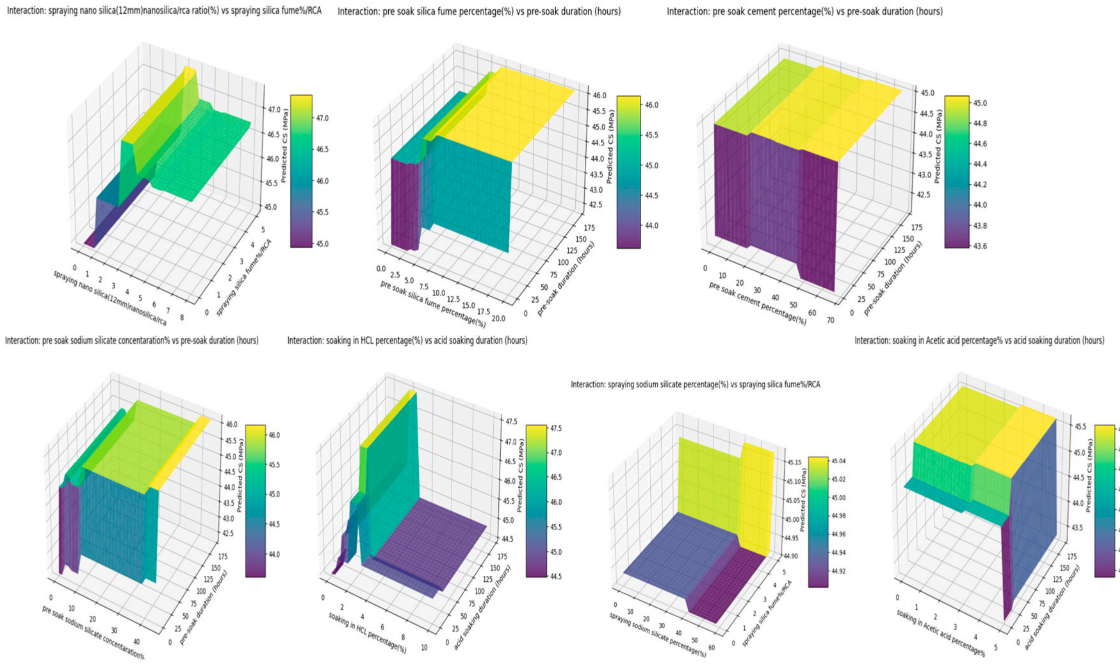

Figure 11. 3D response surfaces for different types of treatment.

In all response surfaces, the high-strength areas remain within constrained ranges of dosage and soaking time, emphasizing that optimal compressive strength is achieved by simultaneously adjusting multiple variables rather than varying each variable individually.

A number of studies have used ML algorithms to develop predictive models for estimating the compressive strength of RAC. However, most previous research focused on untreated RCA; no previous work has incorporated surface treatment characteristics. For example, a previous study on RAC has reported that the R^2 value for the XGBoost model is 0.82 on a dataset, whereas the Random Forest and Gradient Boosting models have significantly lower predictive performance than XGBoost [37]. The study on self-compacting RAC reported R^2 values of 0.7128 and 0.6948 for Random Forest and Gradient Boosting models, respectively, indicating that both models have moderate predictive capacity [35].

However, this study was able to determine XGBoost's R^2 to be 0.909 and establish that Extra Trees have an R^2 of 0.905, indicating superior predictive ability compared to other models. The greater predictive performance observed in this study was made possible through the inclusion of surface treatment parameters and the wider inclusion of various datasets.

6.4. Interpretation of ML Models and Impact of RCA Treatments

The SHAP summary plot in Figure 12 clearly shows the global contribution of input variables to the predicted compressive strength. It is noted that curing age and cement content continue to be the dominant factors; however, several parameters related to the treatment of RCA show a certain degree of influence on the output of the model. It is noted that variables related to the duration of mechanical treatment, acid soaking conditions, pre-soaking duration, and silica-based treatments show a positive influence on the compressive strength of the material; however, the lower degree of influence indicated by the treatment parameters compared to primary variables related to mix design suggests that RCA treatments operate as secondary modifiers. This highlights that treatment effectiveness is strongly dependent on its interaction with the base mix composition and curing conditions.

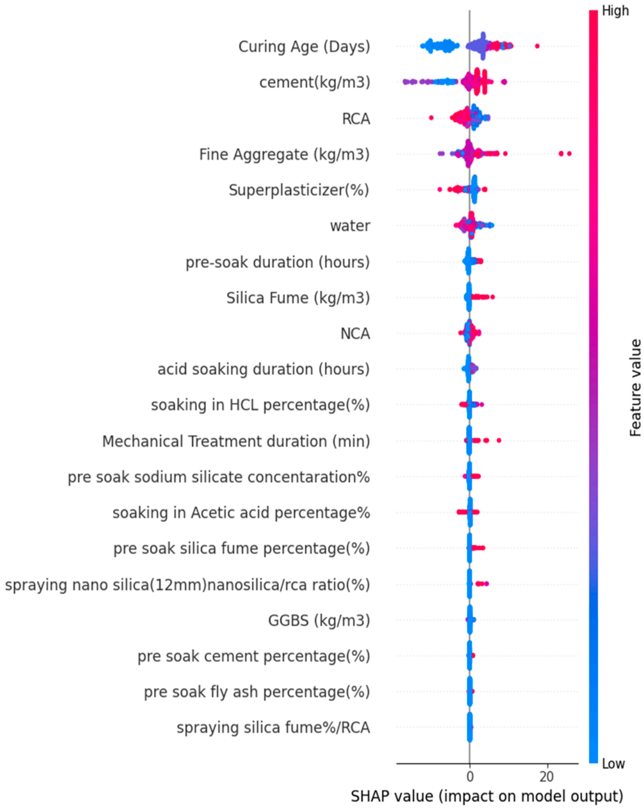

Figure 12. SHAP value for the ET model.

6.5. Integration into a Web Application

To meet the technical demands associated with the estimation of the compressive strength of RAC effectively, a web-based predictive tool has been developed using Python 3.12.13 programming along with the Gradio library. The tool enables users to obtain rapid predictions of the compressive strength using a trained machine learning model. The tool has been trained using experimental data involving variables related to mix proportion variables, aggregate treatment conditions, and mineral additive ratios. The tool's user interface allows users to input 21 variables into four different categories: mix design variables, acid treatment variables, surface treatment variables, and pre-soaking treatment variables. Once the user has entered the variables, the tool's system will process the information using a trained XGBoost algorithm to generate the predicted compressive strength of the recycled aggregate concrete in megapascals (MPa). The tool will be useful to researchers and practitioners to obtain rapid predictions using data before conducting experimental investigations. The developed tool is publicly available at: https://huggingface.co/spaces/marwahtik/RCA_treated (accessed 31 March 2026). Figure 13 shows a screenshot of the RAC compressive strength prediction tool.

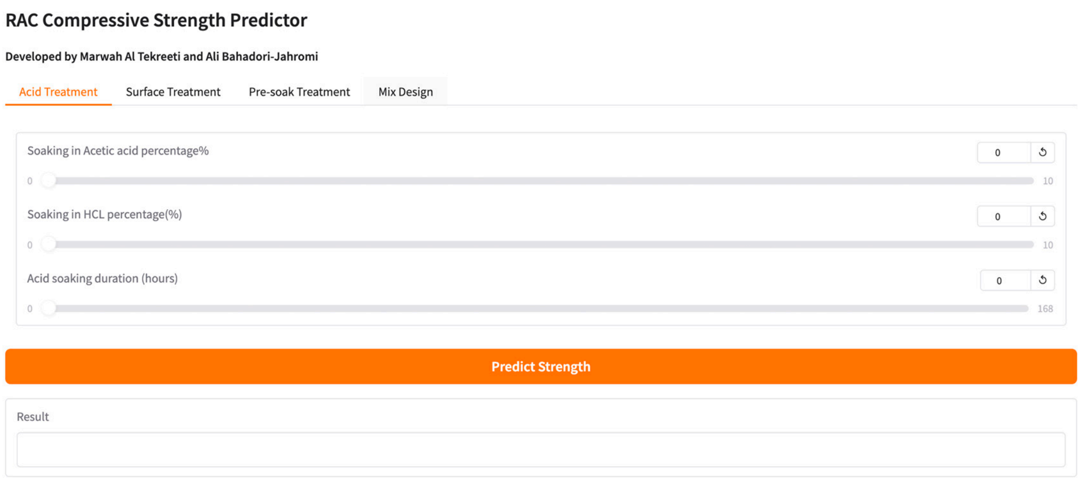

Figure 13. A prediction tool for different RCA treatments.

6.6. Environmental Impact Assessment

Table 9 shows material quantities and corresponding embodied carbon factors used to calculate total CO_2 emissions for each mix. The embodied carbon for all concrete mixes is shown in Figure 14. For each concrete supply chain, environmental assessment was conducted based on a functional unit of 1 m^3 of concrete and using the cradle-to-gate system boundary. The environmental assessment results show that replacing natural aggregates with RCA results in a small reduction in the embodied carbon content of the concrete. Specifically, the embodied carbon content of the NAC is 369.5 kg CO_2/m^3 compared to the RAC, which has an embodied carbon content of 366.4 kg CO_2/m^3. The reduction is due to the lower emissions associated with the use of recycled aggregates compared to the use of natural aggregates, as efforts to extract and process virgin aggregates require more energy and material resources than recycling the concrete from existing structures. Additionally, adding silica fume to untreated RCA produced a slight increase in the embodied carbon content to 367.4 kg CO_2/m^3. However, the increase in embodied carbon is limited because silica fume has a lower emission factor than primary cementitious materials. Therefore, while the use of silica fume resulted in a small amount of additional environmental impact, it provided an increase in compressive strength compared to the RAC control mixture. As a result, the use of supplementary cementitious materials can improve the mechanical properties of the concrete with minimal additional environmental impact.

The various surface treatment methods for RCA were responsible for differing levels of environmental impact. The results show that RAC1 and RAC3 were the two mixes to have the most embodied carbon, 409.9 kg CO_2/m^3 and 414.9 kg CO_2/m^3, respectively. The elevated embodied carbon of these two mixes can be attributed to the use of both acetic acid and sodium silicate in their surface treatment process because both chemistries have higher embodied carbon factors compared to conventional aggregate. Even though the use of chemical surface treatments resulted in an increased environmental burden associated with both RAC1 & RAC3, the treatment processes substantially improved the aggregate quality.

The RAC2 concrete mix exhibited an average embodied carbon of only 372.4 kg CO_2/m^3. This is almost equivalent to that of NAC. It can also be concluded that the use of sodium silicate in the chemical surface treatment process, combined with silica fume or an equivalent, could also be used to improve the performance of RCA while still keeping the environmental impact relatively low.

https://doi.org/10.3390/su18073541

Table 9. Detailed calculation of embodied carbon for each concrete mix.

Mix	Component	Mass (kg/m^3)	Factor (kg CO_2/kg)	CO_2 Contribution (kg/m^3)
NAC	Cement	386	0.91	351.26
	Sand	756	0.005	3.78
	NA	1020	0.005	5.1
	Water	180	0.00034	0.06
	SP	3.86	2.4	9.26
	Total	—	—	369.46
RAC	Cement	386	0.91	351.26
	Sand	756	0.005	3.78
	RCA	1020	0.002	2.04
	Water	230.4	0.00034	0.08
	SP	3.86	2.4	9.26
	Total (base RAC)	—	—	366.42
RAC+SF	Base (RAC)	—	—	366.42
	Water adjustment	2.3	0.00034	0.001
	Silica fume	51	0.02	1.02
	Total	—	—	367.44
RAC1	Base (RAC)	—	—	366.42
	Water correction	−39.0	0.00034	−0.013
	Acetic acid	25	1.7	42.5
	Silica fume	51	0.02	1.02
	Total	—	—	409.93
RAC2	Base (RAC)	—	—	366.42
	Water correction	−36.7	0.00034	−0.012
	Sodium silicate	10	0.5	5
	Silica fume	51	0.02	1.02
	Total	—	—	372.43
RAC3	Base (RAC)	—	—	366.42
	Water correction	−42.8	0.00034	−0.015
	Acetic acid	25	1.7	42.5
	Sodium silicate	10	0.5	5
	Silica fume	51	0.02	1.02
	Total	—	—	414.92

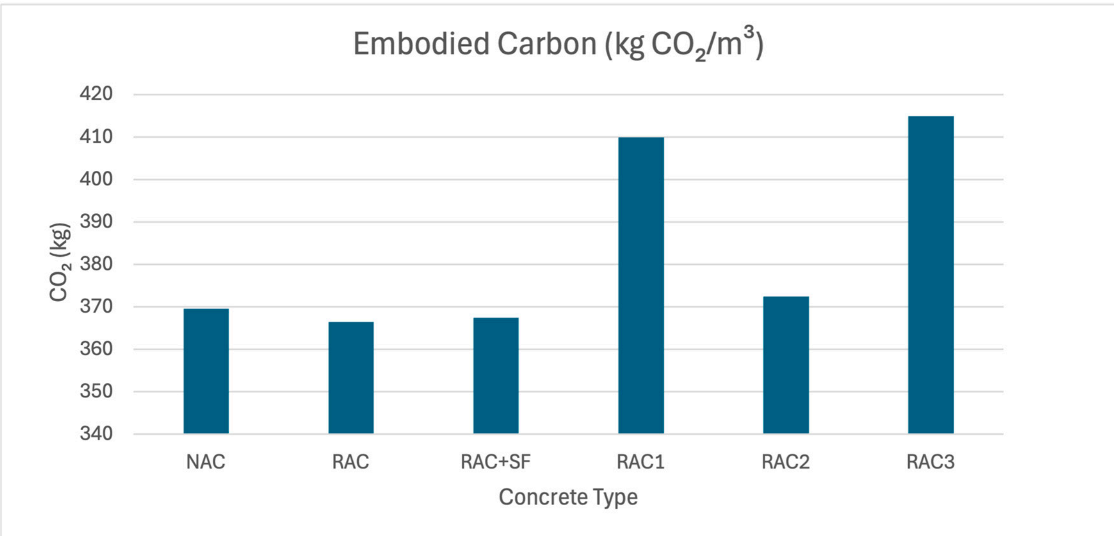

Figure 14. Embodied carbon for different kinds of mixes.

Thus, the concept of the sustainability advantage of treated RCA should be viewed through the lenses of resource savings, waste recycling, and structural performance, rather than the values of carbon savings. The proposed treatment methods for the recycled aggregate would promote the concept of the circular economy by allowing the use of better-quality recycled aggregate to replace natural aggregate.

6.7. Economic Assessment

The estimated production cost of the investigated concrete mixes is presented in Figure 15. The data shows that using RCA instead of NCA dramatically lowers the cost of construction materials. RCA can be purchased for about £30/ton, whereas NCA is typically over twice as expensive. Consequently, recycling construction and demolition (C&D) waste creates a much more cost-effective option for C&D. Although the cost of the RCA + SF mixture increases by adding silica fume to £45/ton, it is still significantly cheaper than NA concrete and has much better mechanical performance than untreated RCA. In addition to raising the cost of RCA by using chemical agents and other surface treatments, RCA will increase the cost of recycling because of the added chemicals applied during treatment. The cost per ton for the treated mixture using acetic acid and silica fume is £60 for RAC1, whereas the cost of RAC2 is marginally lower at £57, while RAC3, being treated with 2 or more agents in total, is the highest at £72 per ton.

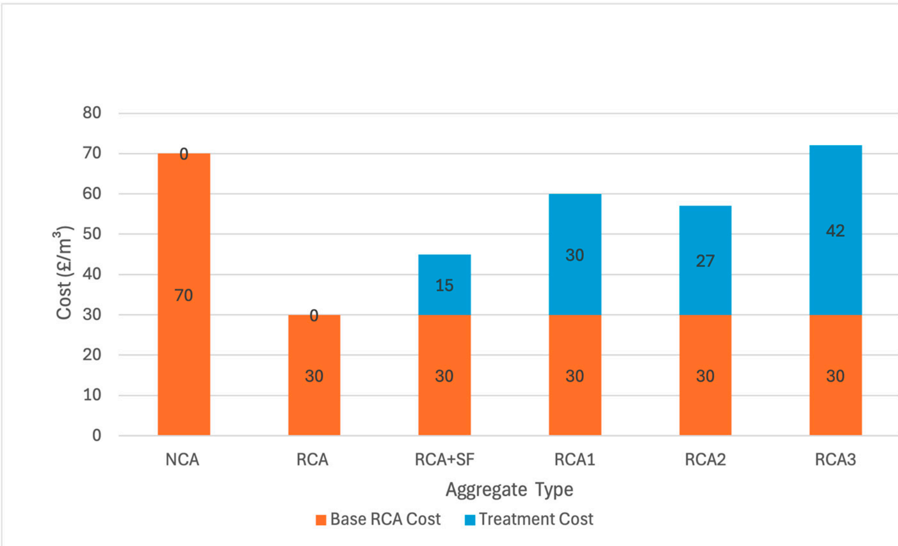

Figure 15. Cost comparison of different aggregate types.

The first of the findings indicates that the economic results derived from RAC1 present an acceptable cost versus strength ratio when measured against the mechanical performance results. While the RAC1 has a higher cost than for untreated RCA mixtures, it is still less expensive than natural aggregate concrete, but offers a compressive strength that is close to that of NCA. Therefore, these findings indicate that treated RCA can be used as an economically feasible and sustainable method of producing concrete.

7. Future Work

1. Larger dataset: Including the span of data on different mix proportions, RCA sources, and curing conditions increases the robustness of models by expanding the database range. Furthermore, with the generation of a greater database, potential bias towards laboratory conditions will be reduced.

2. Inclusion of additional durability parameters: Future research can include durability-based parameters such as chloride resistance, durability, carbonation resistance, and freeze–thaw durability.
3. Multi-objective optimization: Rather than predicting compressive strength alone, future work could focus on optimizing multiple performance indicators such as strength, durability, cost, and carbon footprint. This will better guide the mix and establish a rational relationship between performance and sustainability.
4. Having a more detailed lifecycle analysis, including transportation, building, and end-of-life phases, would help to provide a fuller assessment of how sustainable treated recycled aggregate concrete is over the long term.

8. Conclusions

In this study, the various options for surface treatment of RCA were explored, along with their influence on the mechanical characteristics of RAC, using machine learning-based predictions. The study shows that the use of untreated RCA significantly affects the workability and compressive strength of RAC, mainly due to the material's porosity.

1. Hybrid surface treatments were used to enhance the properties of RCA; the best combination was acetic acid soaking, followed by silica fume spraying RAC1. This surface treatment produced the second-highest compressive strength at 28 days (51.17 MPa) and 90 days (58.34 MPa), which are almost equal to the NAC compressive strength at 28 days (53.16 MPa) and 90 days (58.74 MPa). In addition, sodium silicate hybrid treatments were also able to develop higher compressive strengths than RCA; RAC2 produced 45.67 MPa at 28 days and 51.20 MPa at 90 days, and RAC3 produced 49.75 MPa at 28 days and 55.67 MPa at 90 days. This shows that increasing the compressive strength of modified RCA surfaces will produce greater increases in compressive strength than merely adding silica fume to the concrete mix (RAC+SF: 46.76 MPa at 28 days and 52.80 MPa at 90 days).
2. Among the ML models used to predict RAC compressive strength, XGBoost was found to be the best, with an R^2 of 0.909. The study shows that curing age has a strong influence on the development of concrete compressive strength and cement content. The influence of the RCA treatment parameters was also confirmed to be lower than that of the base mix, a well-established phenomenon.
3. The study shows that an ML-based model can be used to develop a web-based tool for estimating the compressive strength of RAC with minimal computational cost. The tool will be very useful to researchers, helping them reduce their reliance on experimental results.
4. Utilizing RCA reduces the embodied carbon in concrete, though using chemical materials to treat surfaces increases emissions, as more materials are used at this point. The treated mixtures containing RAC2 demonstrated a lower increase in carbon due to being treated, while still providing better performance than untreated aggregates.
5. The cost assessment highlights that RCA is cheaper than NCA, with costs of 70 £ and 30 £, respectively, despite the increased costs due to surface treatment. In general, while surface treatments increase production costs, they also significantly improve the mechanical performance and quality of recycled aggregate concrete, thereby making them viable solutions for sustainable building.

Author Contributions: Conceptualization, M.A.t. and A.B.-J.; methodology, M.A.t.; software, M.A.t. and A.B.-J.; validation, M.A.t.; formal analysis, M.A.t.; investigation, M.A.t.; resources, M.A.t.; data curation, M.A.t.; writing—original draft preparation, M.A.t.; writing—review and editing, M.A.t. and

A.B.-J.; visualization, M.A.t. and A.B.-J. All authors have read and agreed to the published version of the manuscript.

Funding: This research received no external funding.

Institutional Review Board Statement: Not applicable.

Informed Consent Statement: Not applicable.

Data Availability Statement: The data presented in this study are openly available in [Hugging Face] at [https://huggingface.co/spaces/marwahtik/RCA_treated] (accessed 31 March 2026).

Conflicts of Interest: The authors declare no conflicts of interest.

References

1. Global Cement and Concrete Association. 2020. Available online: https://gccassociation.org/concretefuture/cement-concrete-around-the-world/#: :text=14.0%20billion%20m%C2%B3,products%20market%20value%20in%2020202020 (accessed on 25 February 2026).
2. The Department for Environment, Food & Rural Affairs, UK. Statistics on Waste. July 2025. Available online: https://www.gov.uk/government/statistics/uk-waste-data (accessed on 25 February 2026).
3. Tang, Q.; Tian, A.; Ling, C.; Huang, Y.; Gu, F. Physical and mechanical properties of recycled aggregates modified by microbially induced calcium carbonate precipitation. *J. Clean. Prod.* **2022**, *382*, 135409. [CrossRef]
4. Wang, B.; Yan, L.; Fu, Q.; Kasal, B. A Comprehensive Review on Recycled Aggregate and Recycled Aggregate Concrete. *Resour. Conserv. Recycl.* **2021**, *171*, 105565. [CrossRef]
5. Wu, C.; Zhu, Y.; Zhang, X.; Kou, S. Improving the properties of recycled concrete aggregate with bio-deposition approach. *Cem. Concr. Compos.* **2018**, *94*, 248. [CrossRef]
6. Tam, V.W.; Soomro, M.; Evangelista, A.C.J. Quality improvement of recycled concrete aggregate by removal of residual mortar: A comprehensive review of approaches adopted. *Constr. Build. Mater.* **2021**, *288*, 123066. [CrossRef]
7. Yin, J.; Kang, A.; Xiao, P.; Kou, C.; Gong, Y.; Xiao, C. Influences of spraying sodium silicate based solution/slurry on recycled coarse aggregate. *Constr. Build. Mater.* **2023**, *377*, 130924. [CrossRef]
8. Li, L.; Xuan, D.; Chu, S.H.; Lu, J.X.; Poon, C.S. Efficiency and mechanism of nano-silica pre-spraying treatment in performance enhancement of recycled aggregate concrete. *Constr. Build. Mater.* **2021**, *301*, 124093. [CrossRef]
9. Siletani, A.H.; Asayesh, S.; Shirzadi Javid, A.A.; Habibnejad Korayem, A.; Ghanbari, M.A. Influence of coating recycled aggregate surface with different pozzolanic slurries on mechanical performance, durability, and micro-structure properties of recycled aggregate concrete. *J. Build. Eng.* **2024**, *83*, 108457. [CrossRef]
10. Verma, A. Durability and strength characteristics of concrete through various experiments using treated recycled aggregates. *J. Mater. Cycles Waste Manag.* **2025**, *27*, 2321–2340. [CrossRef]
11. Purohit, B.D.; Samaiya, N.K.; Verma, A. Characterisation of recycled aggregate processed through pre-soaking, mechanical grinding and layered coating of aggregates: A three-stage processing technique. *Aust. J. Struct. Eng.* **2025**, *27*, 181–196. [CrossRef]
12. Wang, L.; Wang, J.; Qian, X.; Chen, P.; Xu, Y.; Guo, J. An environmentally friendly method to improve the quality of recycled concrete aggregates. *Constr. Build. Mater.* **2017**, *144*, 432–441. [CrossRef]
13. Al-Bayati, H.K.A.; Das, P.K.; Tighe, S.L.; Baaj, H. Evaluation of various treatment methods for enhancing the physical and morphological properties of coarse recycled concrete aggregate. *Constr. Build. Mater.* **2016**, *112*, 284–298. [CrossRef]
14. Katkhuda, H.; Shatarat, N. Improving the mechanical properties of recycled concrete aggregate using chopped basalt fibers and acid treatment. *Constr. Build. Mater.* **2017**, *140*, 328–335. [CrossRef]
15. Ouyang, K.; Liu, J.; Liu, S.; Song, B.; Guo, H.; Li, G.; Shi, C. Influence of pre-treatment methods for recycled concrete aggregate on the performance of recycled concrete: A review. *Resour. Conserv. Recycl.* **2022**, *188*, 106717. [CrossRef]
16. Wu, C.; Hong, Z.; Zhang, J.; Kou, S. Pore size distribution and ITZ performance of mortars prepared with different bio-deposition approaches for the treatment of recycled concrete aggregate. *Cem. Concr. Compos.* **2020**, *111*, 103631. [CrossRef]
17. Pu, Y.; Li, L.; Wang, Q.; Shi, X.; Luan, C.; Zhang, G.; Fu, L.; Abomohra, A.E. Accelerated carbonation technology for enhanced treatment of recycled concrete aggregates: A state-of-the-art review. *Constr. Build. Mater.* **2021**, *282*, 122671. [CrossRef]
18. Purushothaman, R.; Amirthavalli, R.R.; Karan, L. Influence of treatment methods on the strength and performance characteristics of recycled aggregate concrete. *J. Mater. Civ. Eng.* **2015**, *27*, 04014168. [CrossRef]
19. Peng, Y.; Unluer, C. Analyzing the mechanical performance of fly ash-based geopolymer concrete with different machine learning techniques. *Constr. Build. Mater.* **2022**, *316*, 125785. [CrossRef]
20. Al Tekreeti, M.; Bahadori-Jahromi, A.; Room, S.; Tariq, Z. Optimized Machine Learning Models for Predicting Compressive, Tensile, and Flexural Strengths of Multi-Fiber Recycled Aggregate Concrete. *J. Compos. Sci.* **2026**, *10*, 144. [CrossRef]

21. Peng, Y.; Unluer, C. Modeling the mechanical properties of recycled aggregate concrete using hybrid machine learning algorithms. *Resour. Conserv. Recycl.* **2023**, *190*, 106812. [CrossRef]
22. Marinković, S.; Dragaš, J.; Ignjatović, I.; Tošić, N. Environmental assessment of green concretes for structural use. *J. Clean. Prod.* **2017**, *154*, 633–649. [CrossRef]
23. Xing, W.; Tam, V.W.; Le, K.N.; Butera, A.; Hao, J.L.; Wang, J. Effects of mix design and functional unit on life cycle assessment of recycled aggregate concrete: Evidence from CO_2 concrete. *Constr. Build. Mater.* **2022**, *348*, 128712. [CrossRef]
24. Pradhan, S.; Tiwari, B.R.; Kumar, S.; Barai, S.V. Comparative LCA of recycled and natural aggregate concrete using Particle Packing Method and conventional method of design mix. *J. Clean. Prod.* **2019**, *228*, 679–691. [CrossRef]
25. Marinković, S.; Radonjanin, V.; Malešev, M.; Ignjatović, I. Comparative environmental assessment of natural and recycled aggregate concrete. *Waste Manag.* **2010**, *30*, 2255–2264. [CrossRef]
26. Mostert, C.; Sameer, H.; Glanz, D.; Bringezu, S. Climate and resource footprint assessment and visualization of recycled concrete for circular economy. *Resour. Conserv. Recycl.* **2021**, *174*, 105767. [CrossRef]
27. Xing, W.; Tam, V.W.; Le, K.N.; Hao, J.L. Environmental impacts for recycled aggregate concrete by adopting life cycle assessment (LCA). In *Proceedings of the 25th International Symposium on Advancement of Construction Management and Real Estate*; Springer: Berlin/Heidelberg, Germany, 2020; pp. 13–22.
28. Lovecchio, N.; Shaikh, F.; Rosano, M.; Ceravolo, R.; Biswas, W. Environmental assessment of supplementary cementitious materials and engineered nanomaterials concrete. *AIMS Environ. Sci.* **2020**, *7*, 13. [CrossRef]
29. Martínez-Lage, I.; Vázquez-Burgo, P.; Velay-Lizancos, M. Sustainability evaluation of concretes with mixed recycled aggregate based on holistic approach: Technical, economic and environmental analysis. *Waste Manag.* **2020**, *104*, 9–19. [CrossRef] [PubMed]
30. Yuan, X.; Tian, Y.; Ahmad, W.; Ahmad, A.; Usanova, K.I.; Mohamed, A.M.; Khallaf, R. Machine learning prediction models to evaluate the strength of recycled aggregate concrete. *Materials* **2022**, *15*, 2823. [CrossRef]
31. Ahmed, A.H.A.; Jin, W.; Ali, M.A.H. Comparative analysis of intelligent models for predicting compressive strength in recycled aggregate concrete. *Model. Earth Syst. Environ.* **2024**, *10*, 5273–5291. [CrossRef]
32. Zhang, X.; Dai, C.; Li, W.; Chen, Y. Prediction of compressive strength of recycled aggregate concrete using machine learning and Bayesian optimization methods. *Front. Earth Sci.* **2023**, *11*, 1112105. [CrossRef]
33. Munir, M.J.; Kazmi, S.M.S.; Wu, Y.; Lin, X.; Ahmad, M.R. Development of a novel compressive strength design equation for natural and recycled aggregate concrete through advanced computational modeling. *J. Build. Eng.* **2022**, *55*, 104690. [CrossRef]
34. Imran, H.; Al-Abdaly, N.M.; Shamsa, M.H.; Shatnawi, A.; Ibrahim, M.; Ostrowski, K.A. Development of prediction model to predict the compressive strength of eco-friendly concrete using multivariate polynomial regression combined with stepwise method. *Materials* **2022**, *15*, 317. [CrossRef]
35. de-Prado-Gil, J.; Palencia, C.; Silva-Monteiro, N.; Martínez-García, R. To predict the compressive strength of self compacting concrete with recycled aggregates utilizing ensemble machine learning models. *Case Stud. Constr. Mater.* **2022**, *16*, e01046. [CrossRef]
36. Jagadesh, P.; de Prado-Gil, J.; Silva-Monteiro, N.; Martinez-Garcia, R. Assessing the compressive strength of self-compacting concrete with recycled aggregates from mix ratio using machine learning approach. *J. Mater. Res. Technol.* **2023**, *24*, 1483–1498. [CrossRef]
37. Jadhav, S.P.; Selvam, M.; Zunain, S.M.; Bugalia, N. Evaluating external generalizability of machine learning models for recycled aggregate concrete property prediction. *J. Clean. Prod.* **2024**, *469*, 143166. [CrossRef]
38. Dabiri, H.; Kioumarsi, M.; Kheyroddin, A.; Kandiri, A.; Sartipi, F. Compressive strength of concrete with recycled aggregate; a machine learning-based evaluation. *Clean. Mater.* **2022**, *3*, 100044. [CrossRef]
39. *EN 197-1*; Cement-Part 1: Composition, Specifications and Conformity Criteria for Common Cements. CEN: Brussels, Belgium, 2004.
40. *EN 13263-1*; Silica Fume for Concrete—Part 1: Definitions, Requirements and Conformity Criteria. CEN: Brussels, Belgium, 2005.
41. *BS EN 12620:2002*; Aggregates for Concrete. BSI: London, UK, 2002.
42. Thaue, W.; Iwanami, M.; Nakayama, K.; Yodsudjai, W. Influence of acetic acid treatment on microstructure of interfacial transition zone and performance of recycled aggregate concrete. *Constr. Build. Mater.* **2024**, *417*, 135355. [CrossRef]
43. Verma, A.; Babu, V.S.; Arunachalam, S. Influence of acetic acid soaking and mechanical grinding treatment on the properties of treated recycled aggregate concrete. *J. Mater. Cycles Waste Manag.* **2022**, *24*, 877–899. [CrossRef]
44. *BS EN 12350-2:2009*; Testing Fresh Concrete: Slump-Test. BSI: London, UK, 2009.
45. *BS EN 12390-3*; Testing Hardened Concrete: Compressive Strength of Test Specimens. BSI: London, UK, 2019.
46. Bui, N.K.; Satomi, T.; Takahashi, H. Mechanical properties of concrete containing 100% treated coarse recycled concrete aggregate. *Constr. Build. Mater.* **2017**, *163*, 496. [CrossRef]
47. Lal Chauhan, B.; Jail Singh, G. Sustainable development of recycled concrete aggregate through optimized acid-mechanical treatment: A simplified approach. *Constr. Build. Mater.* **2023**, *399*, 132559. [CrossRef]

48. Sasanipour, H.; Aslani, F.; Taherinezhad, J. Chloride ion permeability improvement of recycled aggregate concrete using pretreated recycled aggregates by silica fume slurry. *Constr. Build. Mater.* **2021**, *270*, 121498. [CrossRef]
49. Alqarni, A.S.; Abbas, H.; Al-Shwikh, K.M.; Al-Salloum, Y.A. Treatment of recycled concrete aggregate to enhance concrete performance. *Constr. Build. Mater.* **2021**, *307*, 124960. [CrossRef]
50. Zhu, L.; Ning, Q.; Han, W.; Bai, L. Compressive strength and microstructural analysis of recycled coarse aggregate concrete treated with silica fume. *Constr. Build. Mater.* **2022**, *334*, 127453. [CrossRef]
51. Wang, J.; Zhang, J.; Cao, D.; Dang, H.; Ding, B. Comparison of recycled aggregate treatment methods on the performance for recycled concrete. *Constr. Build. Mater.* **2020**, *234*, 117366. [CrossRef]
52. Li, L.; Xuan, D.; Sojobi, A.O.; Liu, S.; Chu, S.H.; Poon, C.S. Development of nano-silica treatment methods to enhance recycled aggregate concrete. *Cem. Concr. Compos.* **2021**, *118*, 103963. [CrossRef]
53. Olofinnade, O.M.; Osoata, O.P. Performance assessment of mechanical properties of green normal strength concrete produced with metakaolin-cement coated recycled concrete aggregate for sustainable construction. *Constr. Build. Mater.* **2023**, *407*, 133508. [CrossRef]
54. Ismail, S.; Ramli, M. Engineering properties of treated recycled concrete aggregate (RCA) for structural applications. *Constr. Build. Mater.* **2013**, *44*, 464–476. [CrossRef]
55. Saravanakumar, P.; Abhiram, K.; Manoj, B. Properties of treated recycled aggregates and its influence on concrete strength characteristics. *Constr. Build. Mater.* **2016**, *111*, 611–617. [CrossRef]
56. Singh, P.K.; Rajhans, P. Experimental investigation and SVR model to predict the mechanical properties of RAC by enhancing the characteristic of RCA using surface treatment method along with modified mixing approach. *Constr. Build. Mater.* **2023**, *393*, 132032. [CrossRef]
57. Babalola, O.E.; Awoyera, P.O.; Tran, M.T.; Le, D.; Olalusi, O.B.; Viloria, A.; Ovallos-Gazabon, D. Mechanical and durability properties of recycled aggregate concrete with ternary binder system and optimized mix proportion. *J. Mater. Res. Technol.* **2020**, *9*, 6521–6532. [CrossRef]
58. Gunasekara, C.; Seneviratne, C.; Law, D.W.; Setunge, S. Feasibility of developing sustainable concrete using environmentally friendly coarse aggregate. *Appl. Sci.* **2020**, *10*, 5207. [CrossRef]
59. Gonzalez-Corominas, A.; Etxeberria, M. Effects of using recycled concrete aggregates on the shrinkage of high performance concrete. *Constr. Build. Mater.* **2016**, *115*, 32–41. [CrossRef]
60. Corinaldesi, V. Mechanical and elastic behaviour of concretes made of recycled-concrete coarse aggregates. *Constr. Build. Mater.* **2010**, *24*, 1616–1620. [CrossRef]
61. Breiman, L. Random forests. *Mach. Learn.* **2001**, *45*, 5–32. [CrossRef]
62. Khan, A.; Manan, A.; Umar, M.; Mehmood, M.; Onyelowe, K.C.; Arunachalam, K.P. Enhancing concrete strength for sustainability using a machine learning approach to improve mechanical performance. *Sci. Rep.* **2025**, *15*, 23067. [CrossRef]
63. Schapire, R.E. A brief introduction to boosting. In Proceedings of the 16th International Joint Conference on Artificial Intelligence, Stockholm, Sweden, 31 July–6 August 1999; Volume 99, pp. 1401–1406.
64. Geurts, P.; Ernst, D.; Wehenkel, L. Extremely randomized trees. *Mach. Learn.* **2006**, *63*, 3–42. [CrossRef]
65. Winter, E. The shapley value. In *Handbook of Game Theory with Economic Applications*; Elsevier: Amsterdam, The Netherlands, 2002; Volume 3, pp. 2025–2054.
66. Koffler, C.; Amor, B.; Carbajales-Dale, M.; Cascio, J.; Conroy, A.; Fava, J.A.; Gaudreault, C.; Gloria, T.; Hensler, C.; Horvath, A. On the reporting and review requirements of ISO 14044. *Int. J. Life Cycle Assess.* **2020**, *25*, 478–482. [CrossRef]
67. Blay-Armah, A.; Mohebbi, G.; Bahadori-Jahromi, A.; Fu, C.; Amoako-Attah, J.; Barthorpe, M. Evaluation of embodied carbon emissions in UK supermarket constructions: A study on steel, brick, and timber frameworks with consideration of end-of-life processes. *Sustainability* **2023**, *15*, 14978. [CrossRef]
68. Mohebbi, G.; Bahadori-Jahromi, A.; Ferri, M.; Mylona, A. The role of embodied carbon databases in the accuracy of life cycle assessment (LCA) calculations for the embodied carbon of buildings. *Sustainability* **2021**, *13*, 7988. [CrossRef]
69. Hammond, G.; Jones, C. *Inventory of Carbon & Energy: ICE*; University of Bath: Bath, UK, 2008.
70. *ISO 14044:2006*; Environmental Management-Life Cycle Assessment-Requirements and Guidelines. ISO: Geneva, Switzerland, 2006.

https://doi.org/10.3390/su18073541